
Dirac Delta Regression: Conditional Density Estimation with Clinical Trials

Eric V. Strobl
Vanderbilt University
Nashville, TN

Shyam Visweswaran
University of Pittsburgh
Pittsburgh, PA

Abstract

Personalized medicine seeks to identify the causal effect of treatment for a particular patient as opposed to a clinical population at large. Most investigators estimate such personalized treatment effects by regressing the outcome of a randomized clinical trial (RCT) on patient covariates. The realized value of the outcome may however lie far from the conditional expectation. We therefore introduce a method called *Dirac Delta Regression* (DDR) that estimates the entire conditional density from RCT data in order to visualize the probabilities across all possible treatment outcomes. DDR transforms the outcome into a set of asymptotically Dirac delta distributions and then estimates the density using non-linear regression. The algorithm can identify significant patient-specific treatment effects even when no population level effect exists. Moreover, DDR outperforms state-of-the-art algorithms in conditional density estimation on average regardless of the need for causal inference.

1 The Problem

Randomized clinical trials (RCTs) are the gold standard for inferring causal effects of treatment in biomedicine. These trials utilize the notion of *potential outcomes*, where we consider a treatment variable T with codomain \mathcal{T} and postulate the existence of a random vector $\mathbf{Y} \triangleq (Y(t))_{t \in \mathcal{T}}$ containing the outcomes associated with all possible treatments [23, 28]. We say that T *causes* Y when at least two of the marginal distributions in \mathbf{Y} differ. In an ideal world, we compare the marginals by simultaneously assigning each patient to all treatments \mathcal{T} and then measuring \mathbf{Y} ; in other words, we sample directly from the joint distribution $\mathbb{P}(\mathbf{Y}|\mathcal{T}) = \mathbb{P}(\mathbf{Y})$. However, we can only assign each patient to a single treatment $T = t$ and observe $Y(T = t)$ in practice. We thus can only sample from $\mathbb{P}(Y(T)|T)$, even though we want to sample from the marginals of \mathbf{Y} in order to compare them. RCTs circumvent this problem by randomizing T so that T and \mathbf{Y} are probabilistically independent, or *unconfounded*. The independence implies $\mathbb{P}(Y(t)|T) = \mathbb{P}(Y(t))$ for any $t \in \mathcal{T}$ which in turn implies $\mathbb{P}(Y(T)|T) = \mathbb{P}(Y(T))$. As a result, if we use RCT data to reject the null hypothesis that all distributions in $\{\mathbb{P}(Y(t)|t)\}_{t \in \mathcal{T}}$ are equivalent, then we also reject the null hypothesis that all of the marginal distributions of \mathbf{Y} are equivalent; we can therefore conclude that T causes Y in this case.

Biomedical investigators have traditionally attempted to reject the null of equality in marginals using simple statistics of $Y(T)$ such as the mean (e.g., t-test, ANOVA) or variance (e.g., F-test) which average over patients. However, averages fail to capture patient heterogeneity when patients within the same clinical population respond to treatment differently. For example, all patients with breast cancer do not respond better to the medication raloxifene ($T = 1$) relative to placebo ($T = 0$), but patients who are estrogen or progesterone receptor positive often do [15]; the marginal distributions of $(Y(0), Y(1))$ therefore only differ among breast cancer patients with particular molecular receptors

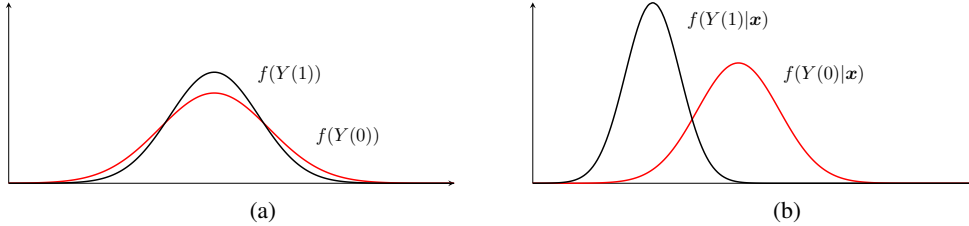


Figure 1: Treatments 0 and 1 are clinically equivalent according to the unconditional densities shown in (a). However, a patient with covariates $\mathbf{X} = \mathbf{x}$ will likely benefit more from treatment 1 as shown by the reduction in symptom severity with the conditional densities in (b).

in this case. Biomedical investigators are thus also interested in computing statistics of $Y(T)$ given a set of patient covariates \mathbf{X} in order to elucidate patient-specific treatment effects.

Most investigators in particular utilize the *conditional mean* obtained by regressing $Y(T)$ on \mathbf{X} (e.g., [36, 14, 35]). The conditional mean however does not capture the uncertainty in treatment effect because it assigns a single point prediction $\hat{\mathbb{E}}(Y(T)|\mathbf{X})$ to each patient. Like many other random variables, the realized treatment effect for a particular patient may lie far from the conditional expectation. As a result, patients and healthcare providers instead prefer to know the conditional probabilities associated with *all* possible values of $Y(T)$ in order to make more informed clinical decisions [1, 5].

Densities can fortunately summarize the desired probabilities in a single intuitive graph. We therefore consider recovering conditional densities $f(Y(T)|\mathbf{X})$ from RCT data. Consider for example two treatments $T = 0$ and $T = 1$. We can estimate the unconditional densities $f(Y(0))$ and $f(Y(1))$ using RCT data as shown in Figure 1 (a). Both of the densities are very similar because they summarize the treatment effect across everyone recruited in the RCT, some of whom may respond well to treatment while others may not. In contrast, Figure 1 (b) displays the densities $f(Y(0)|\mathbf{x})$ and $f(Y(1)|\mathbf{x})$ estimated from the original RCT, as if we had run an RCT personalized towards a particular patient where everyone recruited into the trial had the same covariate values $\mathbf{X} = \mathbf{x}$. Notice that most of the patients in this trial who received $T = 1$ had a reduction in symptom severity Y compared to those who received $T = 0$. Conditional densities thus can summarize the results of a personalized RCT which may differ substantially from the results of the original RCT.

Contributions. In this paper, we propose to recover non-parametric conditional density estimates by utilizing a new procedure called Dirac Delta Regression (DDR). DDR transforms $Y(T)$ into a set of asymptotically Dirac delta distributions and then regresses the distributions on \mathbf{X} as described in Section 3. The algorithm also selects all hyperparameters automatically without access to the true conditional density. We prove consistency of the procedure as well as establish the bias rate with respect to the transformation in Section 4. Experiments in Section 5 show that DDR (a) leads to state-of-the-art performance in practice and (b) allows biomedical investigators to estimate the densities of a personalized RCT from the original RCT data without additional data collection.

2 Related Works

We can estimate non-parametric conditional densities using several other methods besides DDR in order to visualize the probabilities associated with all values of $Y(T)$. Kernel density regression for example estimates $f(Y(T)|\mathbf{X})$ by independently approximating $f(Y(T), \mathbf{X})$ and $f(\mathbf{X})$ using kernel density functions [22, 9, 6]. Other algorithms first estimate the conditional cumulative distribution function (CDF) of $Y(T)$ given \mathbf{X} and then recover the associated density by smoothing the estimated CDF [30, 3]. These two step approaches however degrade accuracy in practice because they incur error in both stages. Investigators therefore later proposed to directly estimate $f(Y(T)|\mathbf{X})$ instead. The earliest methods in this category estimate $f(Y(T)|\mathbf{X})$ by performing expectation-maximization over a mixture of parametric densities [2, 32]. These methods however are very time consuming, and their accuracy depends heavily on the choice of the component densities. [29, 12] thus proposed the Least Squares Conditional Density Estimation (LSCDE) algorithm which estimates $f(Y(T)|\mathbf{X})$ in closed form using reproducing kernels. The authors nevertheless found that LSCDE performs poorly when \mathbf{X} contains multiple variables. Hence, researchers suggested handling the higher dimensional

setting by integrating both dimension reduction and direct density estimation into a single procedure [26, 11, 31]. These methods outperform LSCDE on average when sparsity or a low dimensional manifold exist, but they still struggle to accurately estimate $f(Y(T)|\mathbf{X})$ when the signal does not follow a simple structure. As a result, [10] introduced an algorithm called FlexCode (FC) which utilizes non-linear regression on an orthogonal series (e.g., the Fourier series). FC admits a variety of regression procedures and therefore can capitalize on the successes of regression in high dimensional estimation. Many of the proposed regression procedures however only help FC produce accurate estimates of $f(Y(T)|\mathbf{X})$ in special cases, so it is often unclear how to choose the best regressor in practice. FC also tends to over-smooth its conditional density estimates by enforcing a small number of orthogonal bases. The method therefore can have trouble handling the complexities inherent in real data like its predecessors.

3 Algorithm Design

3.1 Setup

We now provide a detailed description of the DDR algorithm which improves upon FC. We first consider i.i.d. data in the form of triples $\{(\mathbf{x}_i, t_i, y_i(t_i))\}_{i=1}^n$ collected from an RCT. The data corresponds to instantiations of the random variables $(\mathbf{X}, T, Y(T))$, where $Y(T)$ is assumed to be continuous, and \mathbf{X} denotes a vector of covariates measured before we can observe $Y(T)$. We assume that we have $\mathbb{P}(T) > 0$. We also adopt the *strongly ignorable treatment assignment* (SITA) or *unconfoundedness* assumption in the conditional setting which asserts that we have $T \perp\!\!\!\perp \{Y(t)\}_{t \in \mathcal{T}} | \mathbf{X}$ [21, 24]. The SITA assumption holds with an RCT because investigators must assign treatments independently of $Y(T)$ within any stratum of the covariates. The assumption also implies that we have:

$$\mathbb{P}(Y(T)|T, \mathbf{X}) = \mathbb{P}(Y(T)|\mathbf{X}),$$

so that the latter term can be estimated from RCT data. In this paper, we seek to estimate the density $f(Y(t)|\mathbf{X})$ for each treatment value $t \in \mathcal{T}$ using DDR.

3.2 Dirac Delta Regression

Algorithm 1: Dirac Delta Regression (DDR)

Input: training set $\{\mathbf{x}_i, y_i(t)\}_{i=1}^n$, test set $\{\mathbf{x}_i\}_{i=n+1}^m$

Result: conditional density estimates $\mathcal{G}_h \triangleq \{\hat{g}_h(Y(t)|\mathbf{x}_i)\}_{i=n+1}^m$

- 1 Regress Δ_h on \mathbf{X} ; choose the optimal value of h and all other hyperparameters λ using cross-validation with Equation (3)
 - 2 Enforce non-negativity and normalize each element in \mathcal{G}_h using Equation (4)
 - 3 Sharpen each element in \mathcal{G}_h with Equations (5) and (4); choose the optimal value of η again with Equation (3)
-

We design DDR for the setting where $Y(t)$ is continuous because the discrete case is simple. However, it is informative to first consider the discrete setting. Suppose that the discrete variable $Y(t)$ takes on d distinct values in the set $\{z_j\}_{j=1}^d$. Recall that we have $\mathbb{E}[\mathbb{1}(Y(t) = z_k)|\mathbf{X}] = f_{Y(t)}(z_k|\mathbf{X})$ for each $z_k \in \{z_j\}_{j=1}^d$. We can therefore estimate the probability density $f(Y(t)|\mathbf{X})$ by first transforming $Y(t)$ into a set of d indicator functions. In particular, we compute $\mathbb{1}(Y(t) = z_k)$ for each $z_k \in \{z_j\}_{j=1}^d$. With n samples, we thus convert a column vector containing n samples of $Y(t)$ into an $n \times d$ matrix with the i, k^{th} entry corresponding to $\mathbb{1}(y_i(t) = z_k)$. We finally proceed with regressing the set of d indicators on \mathbf{X} to obtain an estimate of $\mathbb{E}[\mathbb{1}(Y(t) = z_k)|\mathbf{X}]$ for each $z_k \in \{z_j\}_{j=1}^d$.

The quantity $\mathbb{1}(Y(t) = z_k)$ is unfortunately almost surely equal to zero in the continuous case. The aforementioned strategy therefore fails in this setting because the $n \times d$ matrix is a matrix of zeros almost surely. Recall however that the following relation holds when $Y(t)$ is continuous [13]:

$$f_{Y(t)}(z_k|\mathbf{X}) = \mathbb{E}[\delta(z_k - Y(t))|\mathbf{X}],$$

where $\delta(z_k - Y(t))$ denotes a Dirac delta distribution, and $\{z_j\}_{j=1}^d$ is now an arbitrary set of values on \mathbb{R} . We can loosely view $\delta(z_k - Y(t))$ as the function equal to infinity on a set of Lebesgue measure zero:

$$\delta(z_k - Y(t)) = \begin{cases} +\infty & \text{if } Y(t) = z_k, \\ 0 & \text{otherwise.} \end{cases}$$

As a result, we cannot transform the response variable into a set of Dirac delta distributions without again obtaining an $n \times d$ matrix of zeros almost surely. We can however “stretch out” the support of the Dirac delta distribution from a single point to an interval by utilizing *asymptotically* Dirac delta distributions δ_h with the stretching parameter h such that $\lim_{h \rightarrow 0^+} \delta_h(z_k - Y(t)) = \delta(z_k - Y(t))$. We in particular choose to utilize a Gaussian density $\delta_h(z_k - Y(t)) = \frac{1}{\sqrt{2\pi}h} \exp\left(-\frac{|z_k - Y(t)|^2}{2h^2}\right)$, although many other densities are also appropriate; we may for example utilize the biweight or tricube density instead. As a general rule, densities with mean zero and lower higher order moments tend to perform better in practice. We can therefore recommend many kernel density functions $\frac{1}{h} K\left(\frac{z_k - Y(t)}{h}\right)$ used in non-parametric unconditional density estimation as well [34]. Regardless of our choice of δ_h , we transform $Y(t)$ into a set of d asymptotically Dirac delta distributions by computing $\delta_h(z_k - Y(t))$ for each $z_k \in \{z_j\}_{j=1}^d$. We therefore convert a column vector containing the n samples of $Y(t)$ into an $n \times d$ matrix with the i, k^{th} entry corresponding to $\delta_h(z_k - y_i(t))$.

Let $\Delta_h = \{\delta_h(z_j - Y(t))\}_{j=1}^d$ denote the set of d asymptotically Dirac delta distributions. DDR then proceeds with non-linear regression of Δ_h on \mathbf{X} using the training set in Step 1. Informally, this strategy approximates the density values at each $z_k \in \{z_j\}_{j=1}^d$ on the test set just like with the discrete case because we have:

$$\lim_{h \rightarrow 0^+} \lim_{n \rightarrow \infty} \widehat{g}_h(z_k | \mathbf{X}) \xrightarrow{p} f_{Y(t)}(z_k | \mathbf{X}), \quad (1)$$

where $\widehat{g}_h(z_k | \mathbf{X}) = \widehat{\mathbb{E}}[\delta_h(z_k - Y(t)) | \mathbf{X}]$ is estimated using a consistent non-linear regression method. We formalize the above intuition in Section 4, where we specifically show that the bias incurred using δ_h instead of δ is of order h^4 under an integrated squared error loss.

3.3 Loss Function & Cross-Validation

We need to choose h carefully because the stretching parameter introduces bias. If we make h too large, then DDR will recover a density that is too flat. On the other hand, if we make the problem too hard with a small h , then the regression procedure will struggle to recover a density that is ultimately “too wiggly.” We therefore must pick h as well as the standard set of hyperparameters of the non-linear regression method λ in a principled manner.

We will choose h and λ using cross-validation. Recall however that we do not have access to the ground truth conditional density $f(Y(t) | \mathbf{X})$. Fortunately, we can utilize a trick by cross-validating over the Mean Integrated Squared Error (MISE) loss function:

$$\begin{aligned} & \int \int \left| \widehat{g}_h(z | \mathbf{x}) - f_{Y(t)}(z | \mathbf{x}) \right|^2 d\mathbb{P}(\mathbf{x}) dz \\ &= \int \int \widehat{g}_h^2(z | \mathbf{x}) d\mathbb{P}(\mathbf{x}) dz - 2 \int \int \widehat{g}_h(z | \mathbf{x}) f_{Y(t)}(z, \mathbf{x}) d\mathbf{x} dz + C, \end{aligned} \quad (2)$$

where C is a constant that only depends on $f(Y(t) | \mathbf{X})$. The empirical MISE loss takes on the following form up to a constant:

$$\sum_{i=1}^n \int \widehat{g}_h^2(z | \mathbf{x}_i) dz - \frac{2}{n} \sum_{i=1}^n \widehat{g}_h(y_i(t) | \mathbf{x}_i). \quad (3)$$

Notice that computing the above quantity does not require knowledge of the ground truth $f(Y(t) | \mathbf{X})$. We therefore can use Equation (3) to tune both h and λ in Step 1 of DDR.

Observe however that we need to estimate $f_{Y(t)}(z | \mathbf{X})$ over all values of z rather than just on the grid $\{z_j\}_{j=1}^d$ to compute Equation (3); we accomplish this task by linearly interpolating between our estimates $\{\widehat{g}_h(z_j | \mathbf{X})\}_{j=1}^d$. Recall that the area under the curve (AUC) of such an interpolated density

converges to the AUC of the true density in any finite interval at rate $O(1/d^2)$ by the trapezoidal rule [4]. We therefore set d to a large number (e.g., 500) and the grid $\{z_j\}_{j=1}^d$ to d equispaced points between the maximum and minimum values of $\{y_i(t)\}_{i=1}^n$ to ensure that the interpolation error is negligible.

3.4 Further Refinements

DDR improves upon the estimate $\hat{g}_h(Y(t)|\mathbf{X})$ in Step 2 by enforcing known properties of a conditional density such as non-negativity and a total AUC of 1; these properties do not automatically hold in the finite sample setting as in unconditional density estimation with kernel density functions. The improved estimate of $f(Y(t)|\mathbf{X})$ thus becomes:

$$\hat{g}_h(Y(t)|\mathbf{X}) \leftarrow \frac{\max\{0, \hat{g}_h(Y(t)|\mathbf{X})\}}{\mathcal{T}(\hat{g}_h(Y(t)|\mathbf{X}))}, \quad (4)$$

where the denominator denotes the total AUC under $\max\{0, \hat{g}_h(Y(t)|\mathbf{X})\}$ as estimated using the trapezoidal rule.

Step 3 of the DDR algorithm further modifies $\hat{g}_h(Y(t)|\mathbf{X})$ using a parameter η by setting:

$$\hat{g}_h(Y(t)|\mathbf{X}) \leftarrow \max\{0, \hat{g}_h(Y(t)|\mathbf{X}) - \eta\}. \quad (5)$$

We choose the optimal η value again using Equation (3). The η value thus serves to eliminate low density regions of $\hat{g}_h(Y(t)|\mathbf{X})$. Re-normalizing $\hat{g}_h(Y(t)|\mathbf{X})$ using Equation (4) then elongates the high density regions. As a result, Equations (5) and (4) together “sharpen” $\hat{g}_h(Y(t)|\mathbf{X})$. In practice, sharpening $\hat{g}_h(Y(t)|\mathbf{X})$ substantially improves performance in the high dimensional setting because it refines the initial conditional density estimates obtained from non-linear regression.

In summary, DDR estimates $f(Y(t)|\mathbf{X})$ by performing non-linear regression on a set of asymptotically Dirac delta distributions. The algorithm then refines the density estimate using Equations (4) and (5). DDR automatically tunes all associated hyperparameters h , λ and η with Equation (3).

4 Theory

We now establish the consistency of DDR as well as the bias of the density estimate as a function of the parameter h . We in particular show that the MISE loss in Equation (2) converges to zero in probability with bias rate $O(h^4)$.

The MISE loss is bounded above by two terms:

$$2 \int \int \left| \hat{g}_h(z|\mathbf{x}) - g_h(z|\mathbf{x}) \right|^2 d\mathbb{P}_{\mathbf{X}}(\mathbf{x}) dz + 2 \int \int \left| g_h(z|\mathbf{x}) - f_{Y(t)}(z|\mathbf{x}) \right|^2 d\mathbb{P}_{\mathbf{X}}(\mathbf{x}) dz$$

The first term corresponds to the *variance* while the second corresponds to the squared *bias*. We require the following assumption for the variance:

Assumption 1. *The regression procedure is consistent for any fixed $h > 0$ and any fixed z :*

$$Q_n(z) \triangleq \int \left| \hat{g}_h(z|\mathbf{x}) - g_h(z|\mathbf{x}) \right|^2 d\mathbb{P}_{\mathbf{X}}(\mathbf{x}) = o_p(1). \quad (6)$$

Many non-parametric regression methods satisfy the above assumption from standard results in the literature. Kernel ridge regression (KRR) for example satisfies it under some mild conditions (Corollary 5 in [27]). K-nearest neighbor, local polynomial, Rodeo and spectral regression also meet the requirement under their respective assumptions [10]. Assumption 1 therefore allows the user to incorporate different regression procedures into DDR.

We next assume that the partial derivative of Q_n w.r.t z is stochastically bounded:

Assumption 2. *$Q_n(z)$ is differentiable w.r.t. z and $\sup_z \left| \frac{\partial Q_n(z)}{\partial z} \right| = O_p(1)$.*

The differentiability of $Q_n(z)$ generally holds when we choose an asymptotically Dirac delta distribution that is everywhere differentiable such as with the aforementioned Gaussian, biweight or tricube

densities. The stochastic bound is equivalent to requiring a finite supremum in the deterministic setting. The assumption therefore ensures a controlled derivative across all values of z .

Now consider the squared bias term:

$$\int \int \left| g_h(z|\mathbf{x}) - f_{Y(t)}(z|\mathbf{x}) \right|^2 d\mathbb{P}_{\mathbf{X}}(\mathbf{x}) dz. \quad (7)$$

The above quantity depends on the choice of the asymptotically Dirac delta distribution as well as the choice of h . We therefore impose some additional assumptions on the distribution:

Assumption 3. *The asymptotically Dirac delta distribution admits the form $\delta_h(z - Y(t)) = \frac{1}{h} K\left(\frac{z - Y(t)}{h}\right)$ such that $\int u K(u) du = 0$ and $\int u^2 K(u) du < \infty$.*

The reader may recall an identical form used in unconditional kernel density estimation, where we also require a centered and finite variance kernel density function [33]. We finally impose a mild smoothness assumption on the density $f(Y(t)|\mathbf{X})$ which is similarly required in the unconditional case:

Assumption 4. *The conditional density $f_{Y(t)}(z|\mathbf{X})$ is twice continuously differentiable for any z and satisfies $\int \int |f''_{Y(t)}(z|\mathbf{x})|^2 d\mathbb{P}_{\mathbf{X}}(\mathbf{x}) dz < \infty$.*

We are now ready to state the main result:

Theorem 1. *Under Assumptions 1-4, we have:*

$$\int_a^b \int \left| \hat{g}_h(z|\mathbf{x}) - f_{Y(t)}(z|\mathbf{x}) \right|^2 d\mathbb{P}_{\mathbf{X}}(\mathbf{x}) dz \leq o_p(1) + Ch^4,$$

for any $a < b$ where C is a constant that does not depend on n or h .

The proof is located in Supplementary Material 7.1. Notice that the above bound holds over all possible finite intervals $[a, b]$ on \mathbb{R} . The parameter h also imposes bias at rate h^4 . We thus achieve consistency as $h \rightarrow 0^+$ as expected from the intuition summarized in Equation (1).

5 Experiments

5.1 Algorithms & Hyperparameters

We next compared DDR against five other algorithms:

1. LSCDE is a least squares procedure for directly estimating the conditional density [29]. This method was shown to outperform two-stage kernel density estimation, but LSCDE in general only performs well with a few variables in \mathbf{X} .
2. Series Conditional Density Estimation (SCDE) improves upon LSCDE in the high dimensional setting by integrating direct conditional density estimation with dimensionality reduction [11].
3. FC estimates conditional densities by utilizing non-linear regression on an orthogonal series [10]. FC admits a variety of regression procedures, so we equipped the algorithm with kernel ridge regression (FC-KRR), k-nearest neighbor (FC-NN) and the Lasso (FC-Lasso).

Recall that we can instantiate DDR with a variety of non-linear regressors like FC. Choosing the right regressor is however a non-trivial task. To prevent the user from cherry picking, we instantiate DDR with KRR with the Gaussian reproducing kernel, a universal regressor that works very well within DDR in the sample size regime of nearly all RCTs (tens to few thousands) [16, 37, 18]. DDR runs in $O(dn^3)$ time in this case, and KRR allows us to compute leave-one-out predictions in closed form via the Sherman-Morrison formula to speed up cross-validation [25]. We selected the h parameter from 50 equispaced points between 0 and 0.5, the ridge penalty from $\{1E-1, 1E-2, 1E-3, 1E-4, 1E-5, 1E-6\}$ and the Gaussian kernel sigma from $\{0.5, 0.8, 1.1, 1.7, 2.0\}$ times the median Euclidean distance between the samples [7, 8]. We will publish the code of DDR along with the camera ready version of this paper. We tuned the hyperparameters of the other algorithms according to the original authors' source codes.

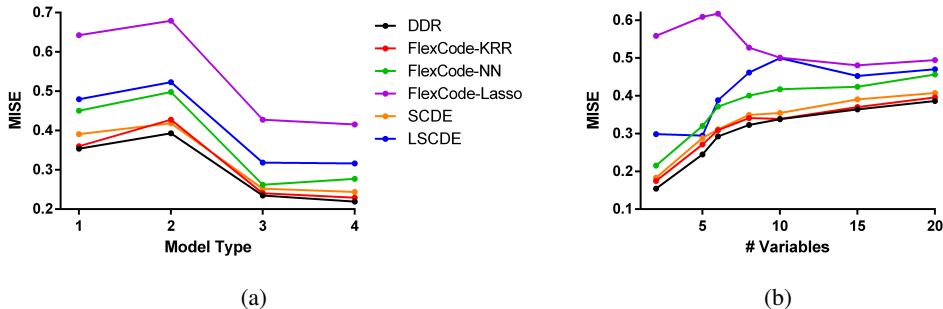


Figure 2: The average MISE loss values as a function of (a) model type and (b) number of variables. DDR achieves the lowest average MISE in all cases.

5.2 Accuracy

Synthetic Data. We first evaluated the six algorithms by simulating experimental datasets with different conditions. Most RCT datasets contain up to a few hundred samples, so we generated 200 samples of $Y(t)$ from the following models: (1) homoskedastic $\mathcal{N}(\mathbf{X}_1, 0.1)$, (2) heteroskedastic $\mathcal{N}(\mathbf{X}_1, 0.1(|\mathbf{X}_2| + 0.5))$, (3) bimodal $\frac{1}{2}\mathcal{N}(\mathbf{X}_1, 0.1) + \frac{1}{2}\mathcal{N}(\mathbf{X}_2, 0.1)$, and (4) skewed $\mathbf{X}_1 + \Gamma(k = 2, \theta = 0.4)$. We instantiated each of the 4 models 100 times. We also set the cardinality of \mathbf{X} to an element of $\{2, 4, 6, 8, 10, 15, 20\}$ by sampling i.i.d. from a standard Gaussian. We therefore compared the algorithms across a total of $4 \times 100 \times 7 = 2800$ datasets.

Since we know the exact ground truth for each sample with the simulated data, we evaluated the algorithms with the true MISE loss in Equation (2) (not just up to a constant) as averaged over the datasets. We summarize the results in Figure 2. DDR achieved the lowest average MISE scores across all four model types (Figure 2 (a)) and all variable numbers (Figure 2 (b)). Moreover, DDR outperformed FC-KRR to a significant degree ($t=-3.89$ $p=1.04E-4$). Every other pairwise comparison was also significant at a Bonferonni corrected threshold of $0.05/6$ according to paired t-tests. FC-Lasso performed the worst, since the linear Lasso is generally not a consistent estimator of the conditional density. We conclude that DDR achieves the best performance on average across a variety of situations.

Real Data. We next ran the algorithm on 40 real observational datasets downloaded from the UCI Machine Learning Repository with sample sizes ranging from 80 to 666. Note that we can only compute the MISE loss up to a constant with the real data because we do not have access to the ground truths. We therefore computed Equation (3) with 10-fold cross-validation and then averaged over the folds for each dataset. Since we cannot compare the loss values between datasets, we ranked the values from 1 to 6 instead. We summarize the results in Table 1 of Supplementary Material 7.2. DDR achieved the lowest average rank across all datasets as shown in the last row. We conclude that the results with the real observational data replicate the results with the synthetic data.

5.3 Clinical Trial Application

We now apply DDR to real RCT data in order to recover conditional densities summarizing treatment effect. The reported discovery is novel even in the medical literature. We investigated the effect of transdermal nicotine patches (TNPs) on long-term smoking cessation using the CTN-0009 dataset from the National Institute of Drug and Alcohol Data Share [19].¹ In this trial, 166 subjects were randomized to receive either TNP or treatment-as-usual (TAU) without TNP over a period of 8 weeks. Smoking increases carbon monoxide (CO) levels in the lung, so the investigators objectively monitored smoking cessation by measuring CO levels with a breathalyzer.

TNPs only mildly increase smoking cessation after treatment ends (Supplementary Material 7.3). The small effect size may exist because only a minority of patients benefit from TNP. We in particular hypothesized that patients who do not consistently smoke the same number of cigarettes experience more intense nicotine cravings than those who do. As a result, patients who do not consistently smoke

¹URL: <https://datashare.nida.nih.gov/study/nida-ctn-0009>

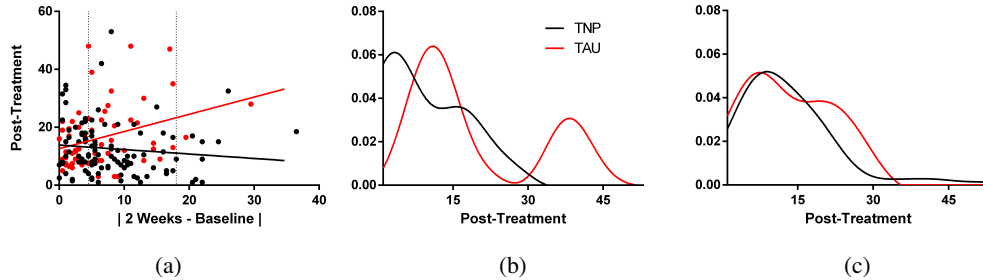


Figure 3: Analysis of a clinical trial dataset for personalized effects of TNP. (a) We can visualize the personalized treatment effect of TNP relative to TAU using two linear regression slopes. (b) The CO levels of this particular patient changed by 18 ppm, so DDR predicts that TNP is more beneficial to this patient than TAU. (c) On the other hand, CO levels only changed by 4.5 ppm in this patient, so DDR could not clearly differentiate the effects of the two treatments.

the same number of cigarettes will benefit more from TNP because TNP decreases the frequency and intensity of the craving episodes [20]. We can evaluate this hypothesis using the RCT dataset, where we track the consistency in smoking using short-term changes in lung CO levels as shown on the x-axis in Figure 3 (a). Based on the two different linear regression slopes, we can see that a change in CO levels while on TNP generally has no effect on post-treatment CO levels but a change in CO levels while on TAU has a detrimental effect.² We confirmed the significance of the observed trend by rejecting the null of equality in slopes between TNP and TAU ($z=-2.87$, one sided $p=0.002$). We therefore conclude that TNP reduces post-treatment CO levels among patients with large changes in short term CO levels.

The regression slopes however only provide point estimates of predicted treatment effect. In reality, even patients with large changes may not benefit from TNP because the post-treatment CO level is stochastic. DDR allows us to visualize this uncertainty by recovering conditional densities. Consider for example patient A with a value of 18 on the x-axis of Figure 3 (a); the regression slopes suggest that this patient is expected to obtain a post-treatment CO level of around 11 if treated with TNP but a level of 23 if treated with TAU. The densities recovered by DDR in Figure 3 (b) for patient A are also significantly different (one sided $p=0.013$; Supplementary Material 7.4), but they imply a more modest effect because the patient also has a high probability of *not* experiencing such a large difference in post-treatment CO levels. On the other hand, patient B with a value of 4.5 on the x-axis is predicted to respond equally well to TNP and TAU in Figure 3 (a); the patient may therefore decide not to take TNP based on the regression estimates. However, DDR recovers broad densities as shown in Figure 3 (c); these densities imply that we cannot differentiate between the two treatments with the available evidence, so patient B may actually benefit more from TNP than TAU. This patient may therefore decide to try TNP after seeing the output of DDR. We conclude that the conditional densities recovered by DDR help patients make more informed treatment decisions by allowing them to visualize the probabilities associated with all possible treatment outcomes in an intuitive fashion.

6 Conclusion

We proposed DDR for estimating conditional densities by performing non-linear regression over a set of asymptotically Dirac delta distributions. DDR outperforms previous methods on average across a variety of synthetic and real datasets. The algorithm also generates patient-specific densities of treatment effect when run on RCT data; as opposed to the conditional expectation, the conditional density recovered by DDR allows patients and healthcare providers to easily compare the probabilities associated with *all* possible treatment outcomes by effectively converting a standard RCT into a personalized one. Theoretical results further support our empirical claims by highlighting the consistency of DDR as well as quantifying the rate of bias with respect to the smoothing parameter h . We ultimately believe that this work is an important contribution to the literature because it introduces a state of the art conditional density estimation method as well as demonstrates a non-trivial application to a real problem in medicine.

²Non-linear polynomial regression produced essentially the same conditional expectation estimates.

References

- [1] A. K. Akobeng. Understanding diagnostic tests 2: likelihood ratios, pre-and post-test probabilities and their use in clinical practice. *Acta paediatrica*, 96(4):487–491, 2007.
- [2] C. M. Bishop. *Pattern recognition and machine learning*. Springer, 2006.
- [3] M. D. Cattaneo, M. Jansson, and X. Ma. Simple local polynomial density estimators. *arXiv preprint arXiv:1811.11512*, 2018.
- [4] D. Cruz-Uribe and C. Neugebauer. An elementary proof of error estimates for the trapezoidal rule. *Mathematics magazine*, 76(4):303–306, 2003.
- [5] G. A. Diamond and J. S. Forrester. Analysis of probability as an aid in the clinical diagnosis of coronary-artery disease. *New England Journal of Medicine*, 300(24):1350–1358, 1979.
- [6] M. Fosgerau and D. Fukuda. Valuing travel time variability: Characteristics of the travel time distribution on an urban road. MPRA Paper 24330, University Library of Munich, Germany, 2010. URL <https://ideas.repec.org/p/pramprapa/24330.html>.
- [7] A. Gretton, K. Borgwardt, M. Rasch, B. Schölkopf, and A. J. Smola. A kernel method for the two-sample-problem. In *Advances in neural information processing systems*, pages 513–520, 2007.
- [8] A. Gretton, K. M. Borgwardt, M. J. Rasch, B. Schölkopf, and A. Smola. A kernel two-sample test. *Journal of Machine Learning Research*, 13(Mar):723–773, 2012.
- [9] R. J. Hyndman, D. M. Bashtannyk, and G. K. Grunwald. Estimating and visualizing conditional densities. *Journal of Computational and Graphical Statistics*, 5(4):315–336, 1996. doi: 10.1080/10618600.1996.10474715. URL <https://amstat.tandfonline.com/doi/abs/10.1080/10618600.1996.10474715>.
- [10] R. Izbicki and A. B. Lee. Converting high-dimensional regression to high-dimensional conditional density estimation. *Electron. J. Statist.*, 11(2):2800–2831, 2017. doi: 10.1214/17-EJS1302. URL <https://doi.org/10.1214/17-EJS1302>.
- [11] R. Izbicki and A. B. Lee. Nonparametric conditional density estimation in a high-dimensional regression setting. *Journal of Computational and Graphical Statistics*, 25(4):1297–1316, 2016. doi: 10.1080/10618600.2015.1094393. URL <https://doi.org/10.1080/10618600.2015.1094393>.
- [12] T. Kanamori, T. Suzuki, and M. Sugiyama. Statistical analysis of kernel-based least-squares density-ratio estimation. *Machine Learning*, 86(3):335–367, 2012.
- [13] R. P. Kanwal. *Generalized functions: theory and applications*. Springer Science & Business Media, 2011.
- [14] A. R. Luedtke and M. J. van der Laan. Statistical inference for the mean outcome under a possibly non-unique optimal treatment strategy. *Ann. Statist.*, 44(2):713–742, 04 2016. doi: 10.1214/15-AOS1384. URL <https://doi.org/10.1214/15-AOS1384>.
- [15] S. Martinkovich, D. Shah, S. L. Planey, and J. A. Arnott. Selective estrogen receptor modulators: tissue specificity and clinical utility. *Clinical interventions in aging*, 9:1437, 2014.
- [16] C. A. Micchelli, Y. Xu, and H. Zhang. Universal kernels. *Journal of Machine Learning Research*, 7(Dec):2651–2667, 2006.
- [17] W. K. Newey and D. McFadden. Chapter 36 large sample estimation and hypothesis testing. volume 4 of *Handbook of Econometrics*, pages 2111 – 2245. Elsevier, 1994. doi: [https://doi.org/10.1016/S1573-4412\(05\)80005-4](https://doi.org/10.1016/S1573-4412(05)80005-4). URL <http://www.sciencedirect.com/science/article/pii/S1573441205800054>.
- [18] M. Noordzij, G. Tripepi, F. W. Dekker, C. Zoccali, M. W. Tanck, and K. J. Jager. Sample size calculations: basic principles and common pitfalls. *Nephrol. Dial. Transplant.*, 25(5): 1388–1393, May 2010.

- [19] M. S. Reid, B. Fallon, S. Sonne, F. Flammino, E. V. Nunes, H. Jiang, E. Kourniotis, J. Lima, R. Brady, C. Burgess, C. Arfken, E. Pihlgren, L. Giordano, A. Starosta, J. Robinson, and J. Rotrosen. Smoking cessation treatment in community-based substance abuse rehabilitation programs. *J Subst Abuse Treat*, 35(1):68–77, Jul 2008.
- [20] J. E. Rose, J. E. Herskovic, Y. Trilling, and M. E. Jarvik. Transdermal nicotine reduces cigarette craving and nicotine preference. *Clinical Pharmacology & Therapeutics*, 38(4):450–456, 1985.
- [21] P. R. Rosenbaum and D. B. Rubin. The central role of the propensity score in observational studies for causal effects. *Biometrika*, 70(1):41–55, 1983.
- [22] M. Rosenblatt. Conditional probability density and regression estimators. *International Symposium on Multivariate Analysis, Multivariate analysis II Proceedings*, 1969.
- [23] D. B. Rubin. Estimating causal effects of treatments in randomized and nonrandomized studies. *Journal of educational Psychology*, 66(5):688, 1974.
- [24] D. B. Rubin. [on the application of probability theory to agricultural experiments. essay on principles. section 9.] comment: Neyman (1923) and causal inference in experiments and observational studies. *Statistical Science*, 5(4):472–480, 1990.
- [25] G. Seber and A. Lee. *Linear Regression Analysis*. Wiley Series in Probability and Statistics. Wiley, 2012. ISBN 9781118274422. URL <https://books.google.com/books?id=X2Y60kX18ysC>.
- [26] M. Shiga, V. Tangkaratt, and M. Sugiyama. Direct conditional probability density estimation with sparse feature selection. *Machine Learning*, 100(2):161–182, Sep 2015. ISSN 1573-0565. doi: 10.1007/s10994-014-5472-x. URL <https://doi.org/10.1007/s10994-014-5472-x>.
- [27] S. Smale and D.-X. Zhou. Learning theory estimates via integral operators and their approximations. *Constructive Approximation*, 26(2):153–172, Aug 2007. ISSN 1432-0940. doi: 10.1007/s00365-006-0659-y. URL <https://doi.org/10.1007/s00365-006-0659-y>.
- [28] J. Splawa-Neyman, D. M. Dabrowska, and T. Speed. On the application of probability theory to agricultural experiments. essay on principles. section 9. *Statistical Science*, pages 465–472, 1990.
- [29] M. Sugiyama, I. Takeuchi, T. Suzuki, T. Kanamori, H. Hachiya, and D. Okanohara. Conditional density estimation via least-squares density ratio estimation. In Y. W. Teh and M. Titterton, editors, *Proceedings of the Thirteenth International Conference on Artificial Intelligence and Statistics*, volume 9 of *Proceedings of Machine Learning Research*, pages 781–788, Chia Laguna Resort, Sardinia, Italy, 13–15 May 2010. PMLR. URL <http://proceedings.mlr.press/v9/sugiyama10a.html>.
- [30] I. Takeuchi, Q. V. Le, T. D. Sears, and A. J. Smola. Nonparametric quantile estimation. *J. Mach. Learn. Res.*, 7:1231–1264, Dec. 2006. ISSN 1532-4435. URL <http://dl.acm.org/citation.cfm?id=1248547.1248592>.
- [31] V. Tangkaratt, N. Xie, and M. Sugiyama. Conditional density estimation with dimensionality reduction via squared-loss conditional entropy minimization. *Neural Computation*, 27:228–254, 2015.
- [32] V. Tresp. Mixtures of gaussian processes. In *Advances in neural information processing systems*, pages 654–660, 2001.
- [33] A. W. v. d. Vaart. *Asymptotic Statistics*. Cambridge Series in Statistical and Probabilistic Mathematics. Cambridge University Press, 1998. doi: 10.1017/CBO9780511802256.
- [34] M. P. Wand and M. C. Jones. *Kernel smoothing*. Chapman and Hall/CRC, 1994.
- [35] B. Zhang, A. A. Tsiatis, M. Davidian, M. Zhang, and E. Laber. Estimating optimal treatment regimes from a classification perspective. *Stat*, 1(1):103–114, 2012.

- [36] B. Zhang, A. A. Tsiatis, E. B. Laber, and M. Davidian. A robust method for estimating optimal treatment regimes. *Biometrics*, 68(4):1010–1018, 2012.
- [37] B. Zhong. How to calculate sample size in randomized controlled trial? *J Thorac Dis*, 1(1): 51–54, Dec 2009.

7 Supplementary Material

7.1 Proofs

Definition 1. (Stochastic equicontinuity w.r.t. z) For every $\varepsilon, \delta > 0$, there exists a sequence of random variables Υ_n and an integer N such that $\forall n \geq N$, we have $\mathbb{P}(|\Upsilon_n| > \varepsilon) < \delta$. Moreover, for each z , there is an open set \mathcal{N} containing z with:

$$\sup_{z' \in \mathcal{N}} |Q_n(z) - Q_n(z')| \leq \Upsilon_n, \quad n \geq N.$$

Notice that Υ_n acts like a random epsilon by bounding changes in $Q_n(z)$ w.r.t. z .

Lemma 1. (Lipschitz continuity \implies stochastic equicontinuity; Lemma 2.9 in [17]) If $Q_n(z) = o_p(1)$ for all $z \in [a, b]$ and $B_n = O_p(1)$ such that for all $z, z' \in [a, b]$ we have $|Q_n(z) - Q_n(z')| \leq B_n |z - z'|$, then $Q_n(z)$ is stochastically equicontinuous w.r.t. z .

Lemma 2. If Assumption 2 holds, then $Q_n(z)$ is stochastically equicontinuous w.r.t. z .

Proof. Because $Q_n(z)$ is differentiable on $[a, b]$ w.r.t. z , we can write:

$$|Q_n(z) - Q_n(z')| \leq \sup_{z \in [a, b]} \left| \frac{\partial Q_n(z)}{\partial z} \right| |z - z'|.$$

We have $\sup_{z \in [a, b]} \left| \frac{\partial Q_n(z)}{\partial z} \right| = O_p(1)$ by Assumption 2. Invoke Lemma 1 to conclude that Q_n is stochastically equicontinuous w.r.t. z . □

Lemma 3. (Stochastic equicontinuity + pointwise consistency \iff uniform consistency; Lemma 2.8 in [17]) We have $Q_n(z) = o_p(1)$ for all $z \in [a, b]$ and $Q_n(z)$ is stochastically equicontinuous w.r.t. z if and only if $\sup_{z \in [a, b]} Q_n(z) = o_p(1)$.

Lemma 4. (Uniform consistency \implies proper integral consistency) If we have $\sup_{z \in [a, b]} Q_n(z) = o_p(1)$, then $\int_a^b Q_n(z) dz = o_p(1)$.

Proof. Choose $\varepsilon > 0$. Then write:

$$\begin{aligned} \mathbb{P}\left(\left|\int_a^b Q_n(z) dz\right| \geq \varepsilon\right) &\leq \mathbb{P}\left(\int_a^b |Q_n(z)| dz \geq \varepsilon\right) \\ &\leq \mathbb{P}\left(\int_a^b \sup_{z \in [a, b]} |Q_n(z)| dz \geq \varepsilon\right) \\ &= \mathbb{P}\left((b-a) \sup_{z \in [a, b]} |Q_n(z)| \geq \varepsilon\right) \\ &= \mathbb{P}\left(\sup_{z \in [a, b]} |Q_n(z)| \geq \frac{\varepsilon}{b-a}\right). \end{aligned} \tag{8}$$

Choose $\delta > 0$. By assumption, for $\frac{\varepsilon}{b-a}$ and δ , $\exists N \in \mathbb{N}^+$ such that $\forall n \geq N$, we have:

$$\mathbb{P}\left(\sup_{z \in [a, b]} |Q_n(z)| \geq \frac{\varepsilon}{b-a}\right) \leq \delta.$$

Note that we chose ε and δ arbitrarily. The conclusion follows by the epsilon-delta definition of convergence in probability to zero. □

Theorem 1. Under Assumptions 1-4, we have:

$$\int_a^b \int \left| \widehat{g}_h(z|\mathbf{x}) - f_{Y(t)}(z|\mathbf{x}) \right|^2 d\mathbb{P}_{\mathbf{X}}(\mathbf{x}) dz \leq o_p(1) + Ch^4,$$

for any $a < b$ where C is a constant that does not depend on n or h .

Proof. We write:

$$\begin{aligned} & \int_a^b \int \left| \widehat{g}_h(z|\mathbf{x}) - f_{Y(t)}(z|\mathbf{x}) \right|^2 d\mathbb{P}_{\mathbf{X}}(\mathbf{x}) dz \\ & \leq 2 \int_a^b \int \left| \widehat{g}_h(z|\mathbf{x}) - g_h(z|\mathbf{x}) \right|^2 d\mathbb{P}_{\mathbf{X}}(\mathbf{x}) dz + 2 \int_a^b \int \left| g_h(z|\mathbf{x}) - f_{Y(t)}(z|\mathbf{x}) \right|^2 d\mathbb{P}_{\mathbf{X}}(\mathbf{x}) dz \end{aligned} \quad (9)$$

The term $Q_n(z) = \int \left| \widehat{g}_h(z|\mathbf{x}) - g_h(z|\mathbf{x}) \right|^2 d\mathbb{P}_{\mathbf{X}}(\mathbf{x})$ is $o_p(1)$ for each $z \in [a, b]$ by Assumption 1. Invoke Lemmas 2, 3 and then 4 to conclude that we have:

$$\int_a^b \int \left| \widehat{g}_h(z|\mathbf{x}) - g_h(z|\mathbf{x}) \right|^2 d\mathbb{P}_{\mathbf{X}}(\mathbf{x}) dz = o_p(1).$$

We now focus on the term $\left| g_h(z|\mathbf{x}) - f_{Y(t)}(z|\mathbf{x}) \right|^2$. We write:

$$\begin{aligned} g_h(z|\mathbf{x}) - f_{Y(t)}(z|\mathbf{x}) &= \int \frac{1}{h} K\left(\frac{z-k}{h}\right) f_{Y(t)}(k|\mathbf{x}) dk - f_{Y(t)}(z|\mathbf{x}) \\ &= \int K(u) \left(f_{Y(t)}(z-hu|\mathbf{x}) - f_{Y(t)}(z|\mathbf{x}) \right) du. \end{aligned} \quad (10)$$

We then utilize a Taylorian expansion with a Laplacian representation of the remainder:

$$f_{Y(t)}(z+hu|\mathbf{x}) - f_{Y(t)}(z|\mathbf{x}) = hf'_{Y(t)}(z|\mathbf{x}) + h^2 \int_0^1 f''_{Y(t)}(z+sh|\mathbf{x})(1-s) ds.$$

Substituting the above formula into Equation (10), we get:

$$\begin{aligned} & g_h(z|\mathbf{x}) - f_{Y(t)}(z|\mathbf{x}) \\ &= \int \int_0^1 K(u) [-hu f'_{Y(t)}(z|\mathbf{x}) + h^2 u^2 f''_{Y(t)}(z-shu|\mathbf{x})(1-s)] ds du \\ &= \int \int_0^1 h^2 u K(u) \left(u f''_{Y(t)}(z-shu|\mathbf{x})(1-s) \right) ds du, \end{aligned} \quad (11)$$

where the second equality follows because we assumed that K has expectation zero. We next utilize the Cauchy-Schwartz inequality $(\mathbb{E}AB)^2 \leq \mathbb{E}A^2 \mathbb{E}B^2$ with $A = U$ and $B = U f''(z - ShU|\mathbf{x})(1 - S)$; here U has density K and S is uniform on $[0, 1]$ as well as independent of U . The bottom of Equation (11) squared is therefore upper bounded by:

$$\begin{aligned} & h^4 \int K(u) u^2 du \int \int_0^1 K(u) u^2 f''_{Y(t)}(z-shu|\mathbf{x})^2 (1-s)^2 ds du \\ &= h^4 \int K(u) u^2 du \int \int_0^1 K(u) u^2 f''_{Y(t)}(z|\mathbf{x})^2 (1-s)^2 ds du \\ &= h^4 \left(\int K(u) u^2 du \right)^2 f''_{Y(t)}(z|\mathbf{x})^2 \frac{1}{3}. \end{aligned}$$

Integrating this with respect to $\mathbb{P}_{\mathbf{X}}(\mathbf{x})$ and z , we obtain:

$$\begin{aligned} & \int_a^b \int \left(g_h(z|\mathbf{x}) - f_{Y(t)}(z|\mathbf{x}) \right)^2 d\mathbb{P}_{\mathbf{X}}(\mathbf{x}) dz \\ & \leq h^4 \left(\int K(u) u^2 du \right)^2 \frac{1}{3} \int_a^b \int f''_{Y(t)}(z|\mathbf{x})^2 d\mathbb{P}_{\mathbf{X}}(\mathbf{x}) dz. \end{aligned}$$

We finally utilize the bound in Equation (9) to conclude that:

$$\int_a^b \int \left| g_h(z|\mathbf{x}) - f_{Y(t)}(z|\mathbf{x}) \right|^2 d\mathbb{P}_{\mathbf{X}}(\mathbf{x}) dz \leq o_p(1) + Ch^4,$$

where $C = \left(\int K(u) u^2 du \right)^2 \frac{2}{3} \int_a^b \int f''_{Y(t)}(z|\mathbf{x})^2 d\mathbb{P}_{\mathbf{X}}(\mathbf{x}) dz$. \square

	(rank)	DDR	FC-KRR	FC-NN	FC-Lasso	SCDE	LSCDE
Autism	5	-1.85E-01	-7.25E-01	-8.92E-01	-2.40E-01	-8.00E-01	-3.63E-02
AutoMPG	3	-6.20E-02	-7.28E-02	-1.02E-01	+3.38E-02	+5.63E-02	-5.30E-02
Breast	1	-5.31E+00	-5.08E+00	-3.94E+00	-2.18E+00	+4.16E+00	-3.13E+00
BuddyMove	4	-1.67E-02	-2.21E-02	-2.63E-02	+3.18E-03	+5.13E-03	-1.69E-02
Caesarian	4	-2.58E-02	-1.85E-02	-3.18E-02	+2.10E-01	-1.06E-01	-2.74E-02
CKD	1	-4.80E-03	-4.69E-03	-4.65E-03	-2.54E-03	-2.76E-04	-3.22E-03
Coimbra	1	-3.54E-02	-3.11E-02	-2.41E-02	-2.54E-02	+2.05E-01	-2.19E-02
Concrete	1	-3.65E-02	-3.36E-02	-2.56E-02	-1.83E-02	+6.43E-02	-3.53E-02
Credit	1	-1.68E-02	-1.55E-02	-1.56E-02	-1.00E-02	-6.05E-03	-1.48E-02
Cryotherapy	3	-7.47E-03	-6.31E-03	-2.94E-03	-7.94E-03	-1.87E-02	-1.99E-03
CSM	1	-8.90E-08	-8.35E-08	-7.02E-08	-1.43E-08	-1.51E-08	-6.40E-08
Dermatology	2	-9.40E-03	-8.38E-03	-8.54E-03	-9.31E-03	-1.00E-02	-8.75E-03
Echo	5	-3.64E+00	-7.95E+00	-7.03E+00	-6.54E+00	-5.93E+00	-7.63E-01
EColi	1	-1.16E+00	-1.10E+00	-1.06E+00	-7.57E-01	-1.06E+00	-1.12E+00
Facebook	2	-7.05E-05	-7.93E-05	-6.04E-05	-8.30E-06	-3.18E-06	-3.82E-05
Fertility	4	-1.08E+00	-1.19E+00	-4.03E+00	+6.37E+00	-4.59E+00	-9.80E-02
ForestFires	2	-1.40E-01	-1.08E-01	-9.99E-02	-2.48E-02	-1.86E-01	-9.66E-02
ForestTypes	1	-2.52E-02	-2.35E-02	-2.20E-02	-9.02E-03	-1.19E-02	-2.32E-02
Glass	1	-2.14E+02	-1.83E+02	-1.57E+02	-2.67E+01	-1.48E+02	-1.95E+02
GPS	2	-6.61E-02	-4.12E-02	-3.73E-02	+1.61E-03	-2.83E-02	-8.52E-02
Hayes	4	-3.05E-03	-3.27E-03	-3.57E-03	-3.67E-03	-2.88E-03	-2.53E-03
HCC	1	-5.89E-01	-5.04E-01	-5.54E-01	-1.60E-01	+1.67E-01	-4.07E-01
Hepatitis	1	-1.16E-02	-1.05E-02	-1.09E-02	-9.80E-03	-7.10E-03	-1.04E-02
Immunotherapy	1	-5.88E-02	-5.80E-02	-5.11E-02	+8.88E-02	+7.88E-02	-5.22E-02
Inflammation	1	-2.21E-01	-2.20E-01	-2.04E-01	-1.30E-01	-1.98E-01	-1.86E-01
Iris	4	-3.64E-01	-4.89E-01	-5.14E-01	-3.66E-02	-6.98E-01	-3.01E-01
Istanbul	2	-1.97E+01	-2.04E+01	-1.75E+01	-8.64E+00	-1.43E+01	-1.75E+01
Leaf	2	-3.77E+00	-4.07E+00	-3.32E+00	-1.65E+00	-3.24E+00	-2.10E+00
Parkinson's	1	-2.08E-02	-1.90E-02	-1.24E-02	-4.70E-03	-3.53E-03	-1.13E-02
Planning	2	-5.45E-01	-5.21E-01	-3.47E-01	-2.90E-01	-5.03E-01	-9.38E-01
Seeds	1	-1.66E-02	-1.49E-02	-1.20E-02	-4.52E-03	-1.33E-02	-1.38E-02
Somerville	4	-2.77E+00	-5.78E+00	-7.26E+00	-7.00E+00	-1.11E+00	-2.27E+00
SPECTF	1	-2.32E-02	-2.24E-02	-2.14E-02	-2.13E-02	+4.03E-02	-1.89E-02
Statlog	4	-7.03E-03	-7.71E-03	-1.45E-02	+2.10E-02	+9.83E-03	-7.85E-03
Thoracic	2	-1.97E-01	-1.77E-01	-1.64E-01	-1.11E-01	-2.37E-01	-1.53E-01
Traffic	6	-2.72E-02	-2.17E-01	-6.30E-01	-6.13E-01	-6.38E-01	-4.75E-02
User	2	-6.51E-01	-6.16E-01	-5.96E-01	+4.01E-01	-7.08E-01	-5.11E-01
Wine	2	-8.55E-04	-8.63E-04	-7.41E-04	-2.18E-04	-4.14E-04	-6.77E-04
Wisconsin	3	-1.16E-01	-1.18E-01	-9.61E-02	-5.74E-02	-1.38E-01	-6.45E-02
Yacht	2	-1.03E-01	-1.27E-01	-9.58E-02	+1.39E-02	-9.68E-02	-6.33E-02
Avg. Rank		2.28	2.55	3.08	5.03	4.05	4.03

Table 1: Results from 40 real observational datasets. Lower MISE loss values (up to a constant) denote better performance. The second column lists the rank of DDR relative to the other algorithms. DDR performs the best on average by achieving the lowest average rank as shown in the last row.

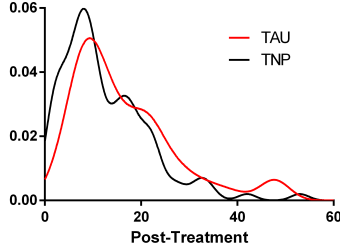


Figure 4: The unconditional densities estimated by standard kernel density estimation. The TNP density is shifted slightly to the left relative to the TAU density.

7.2 Real Data Results

We have summarized the results with real data in Table 1.

7.3 Extra Clinical Trial Results

TNPs only mildly increase smoking cessation after treatment ends. We can verify this claim by plotting the estimated unconditional densities of CO levels measured 9 weeks after completion of TNP or TAU treatment (kernel density estimation with Gaussian kernel function and unbiased cross-validation; Figure 4). Notice that the TNP density is shifted to the left relative to the TAU density, indicating that patients treated with TNP eventually smoke less than those treated with TAU on average. The difference is small at 3.97 ppm but large enough to reject the null of equality in means using a t-test ($t=-2.369$, $p=0.020$).

7.4 Hypothesis Testing

The TNP density in Figure 3 (b) places higher probability at lower post-treatment CO levels than the TAU density. DDR may nevertheless recover such densities often when the TNP density does *not* place higher probability at lower post-treatment CO levels at the population level. We therefore also seek to reject the following null hypothesis:

$$H_0 : \sup_z \left[F_{Y(1)}(z|\mathbf{x}) - F_{Y(0)}(z|\mathbf{x}) \right] \leq 0,$$

where $F_{Y(t)}(z|\mathbf{X}) = \int_{-\infty}^z f_{Y(t)}(u|\mathbf{X}) du$. Notice that larger values of the above difference correspond to concentration of probability at lower values of z . We therefore reject the null when the difference is large because lower values of z correspond to reduced post-treatment CO levels. We implement the hypothesis test by permuting the treatment labels with the following conditional statistic:

$$\mathcal{S} = \sup_z \left[\hat{F}_{h,Y(1)}(z|\mathbf{x}) - \hat{F}_{h,Y(0)}(z|\mathbf{x}) \right],$$

where $\hat{F}_{h,Y(t)}(z|\mathbf{X}) = \int_{-\infty}^z \hat{g}_{h,Y(t)}(u|\mathbf{X}) du$. We obtained a p-value of 0.0125 with 2000 permutations for patient A by setting $T = 0$ to TAU and $T = 1$ to TNP. We thus reject H_0 in this case and conclude that the TNP density places higher probability at lower post-treatment CO levels than the TAU density. Repeating the same process with patient B on the other hand led to a p-value of 0.3635.